LOW PHASE-NOISE UHF THIN-FILM PIEZOELECTRIC-ON-SUBSTRATE LBAR OSCILLATORS

H. M. Lavasani, R. Abdolvand, and F. Ayazi*
School of ECE, Georgia Institute of Technology, Atlanta, Georgia, USA
(*now with the School of ECE, Oklahoma State University, Oklahoma, USA)

ABSTRACT

This paper reports on the first demonstration of a low phase-noise 467MHz temperature-compensated oscillator based on a ZnO-on-nanocrystalline diamond lateral bulk acoustic resonator (LBAR). The temperature compensation is achieved by using a thin silicon-dioxide buffer layer on the surface of the diamond film. The oscillator performance is compared with an uncompensated 496MHz AlN-on-silicon oscillator. The sustaining circuitry is comprised of a 9.4mW tunable transimpedance amplifier (TIA) in 0.18µm CMOS. The phase-noise is measured below −80dBc/Hz at 1kHz offset with temperature drift of < −4ppm/ºC from -5ºC to 90ºC.

1. INTRODUCTION

Frequency reference oscillator is a key block in any modern radio transceiver. Reference oscillators based on high quality factor (Q) micromechanical resonators are gaining currency as an alternative to quartz crystal oscillators due to their small form factor and potential integration with IC. Currently, most reference oscillators operate in the VHF range [1], [2]. However, as the carrier frequency increases, the larger up-conversion ratio in frequency synthesizers limits the performance of the front-end. Recent advances in micromachining technology have made the realization of UHF micromachined oscillators possible [3].

UHF micromechanical resonators, either exhibit significantly high motional impedance (>1kΩ) when using capacitive transduction or low Q (<1,000) when using piezoelectric transduction and operating in thickness-mode. These issues make the realization of a low phase-noise low-power oscillator challenging. Thin-film piezoelectric-on-substrate (TPoS) resonators are viable solution to address these deficiencies. The motional impedance of TPoS resonators are usually orders of magnitude lower than capacitively-transduced resonators at the same frequency which simplifies the sustaining circuitry. Moreover, the TPoS resonators do not require a polarization voltage (as opposed to capacitive resonators) and most importantly they can be operated in atmospheric pressure. Since the substrate is made of high-energy-density materials, TPoS resonators also offer superior power handling which in-turn improves the phase-noise performance of the oscillator.

In this paper, a low phase-noise 467MHz *temperature-compensated* oscillator based on a ZnO-on-nanocrystalline diamond LBAR (R_m~600Ω , Q~1,850 in air) is demonstrated and compared with an *uncompensated* 496MHz AlN-on-silicon LBAR (R_m~650Ω, Q~3,800 in air) oscillator. Both resonators were fabricated in Georgia Tech's Microelectronics Research Center. The sustaining circuitry for both oscillators consists of a three-stage 0.18µm CMOS tunable TIA that consumes 6.2mA from a 1.5V supply. The measured phase-noise of the 467MHz resonator at 1kHz is -80dBc/Hz with temperature coefficient of frequency (TCF) below −4ppm/ºC. The reduction in TCF is significant as it constitutes 9× improvements over an uncompensated piezoelectric-on-silicon oscillator. The phase-noise of 496MHz oscillator at 1kHz offset measures less than −92dBc/Hz. This oscillator meets the GSM phase-noise requirement.

2. OSCILLATOR BLOCK DIAGRAM

The block diagram of the reference oscillator is shown in Fig. 1. The frequency of oscillation is determined by either a ZnO-on-nanocrystalline diamond or AlN-on-Silicon LBAR resonator. The sustaining amplifier consists of two parts: transimpedance amplifier with tunable gain and two subsequent voltage amplifiers. The gain tuning is achieved by an NMOS resistor. Due to large power-handling of these resonators (>0dBm), automatic level control (ALC) is not necessary.

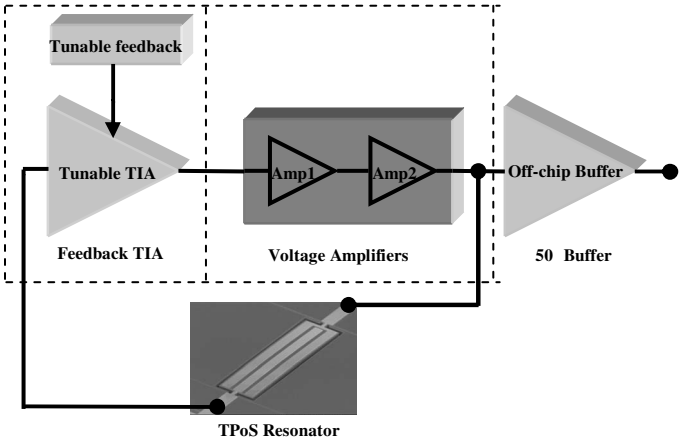

Fig. 1: Block diagram of the LBAR oscillator.

3. LBAR RESONATOR SPECIFICATION

The 467MHz resonator used in this work is a 3rd order LBAR. Two to three micrometer of nanocrystalline diamond (NCD) is deposited on a silicon handle wafer to prepare the initial substrate. The process flow for fabrication of these devices is described elsewhere [4]. An oxide buffer layer is initially deposited on top of the relatively rough NCD surface and is polished back to provide for a smooth surface. Although this polished thin oxide film slightly degrades the effect of diamond on increasing the resonance frequency of the structure, it is necessary for the operation of the resonator.

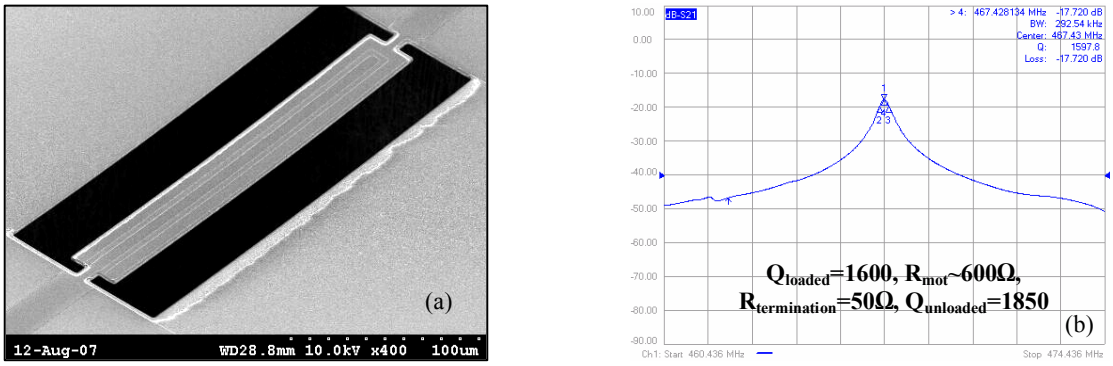

Fig. 2: (a) SEM view, (b) Frequency response of the 467MHz ZnO-on-nanocrystalline diamond LBAR

This is because the slightest roughness in the starting substrate can significantly deteriorate the quality of the piezoelectric film sputtered onto the surface [5]; since polishing the diamond layer is not a trivial task our alternative method is practically valuable. Moreover, the oxide layer will reduce the effective temperature coefficient of frequency (TCF) of the composite resonant structure [4]. The frequency response plot and the SEM picture of the ZnO-on-diamond resonator are shown in Fig. 2. All the measurements in this work are performed on a Suss high frequency probe station and cascade GSG probes are used to connect the device to an Agilent E8364B vector network analyzer. The motional impedance of the resonator is <600Ω and the unloaded Q is ~1,850 in air.

The utilized AlN-on-silicon resonator, on the other hand, is a 9th order LBAR fabricated on a 10μm thick silicon-on-insulator (SOI) substrate. The AlN film is 1μm thick and the process flow is essentially the same as the one developed for ZnO-in-silicon devices earlier [6]. The bottom electrode for this device is made of Mo and the AlN in etched in chlorine plasma to define the resonator structure. Access to the bottom electrodes are made possible by chemically etching the AlN film on top of the ground pads, and the top electrode are made of e-beam evaporated Al film. The corresponding frequency response of the AlN-on-silicon resonator is shown in Fig 3. The motional impedance of the resonator is <650Ω and the unloaded Q is ~ 3,800 in air.

The starting substrates in both of the devices explained above are made of low acoustic loss materials which are intended to improve the structural integrity and the quality factor of the resonant structure. Additionally, the effective stiffness of a TPoS resonator which comprises of a relatively thick substrate is higher than a device made of a thin piezoelectric material only. Therefore the power density of the resonator is improved [7] and a better phase noise density is expected for the oscillator built with these devices. Based on the same argument we can conclude that a thicker substrate will further improve the power handling and the phase noise characteristic. However, it should be noted that increasing the thickness will also cause the motional impedance of the resonator to gradually increase which is not favorable in oscillator application. According to this discussion between the two resonators introduced in this section the latter is expected to have higher power density.

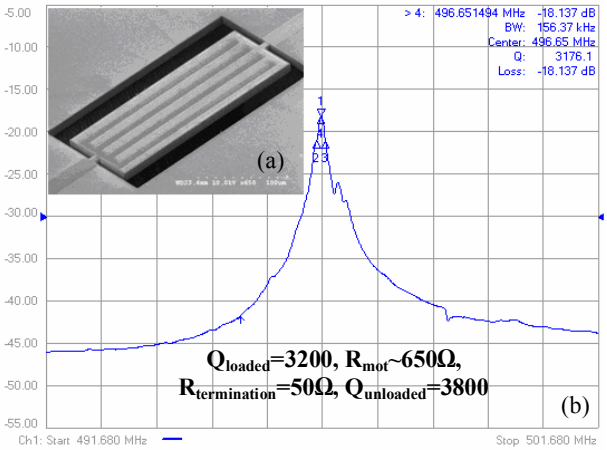

Fig. 3: (a) SEM view, (b) Frequency response of the 496MHz AlN-on-Silicon LBAR.

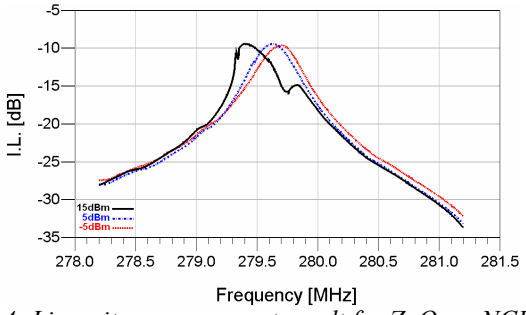

Fig. 4: Linearity measurement result for ZnO-on-NCD

Linearity measurement has been performed on the resonators fabricated on the two substrates and results are compared. The frequency responses measured from a ~280MHz device fabricated on the diamond substrate with variable applied input power level from -5dBm up to 15dBm are overlapped in Fig. 4. These measurements are repeated on a device with the same geometry fabricated on the 10μm SOI substrate (Fig. 5). The resonance frequency of the AlN-on-silicon resonator is lower and the motional impedance is larger as expected. The ZnO-on-NCD resonator shows clear signs of nonlinear behavior at 15dBm whereas the frequency response of the AlN-on-silicon device is not visibly altered.

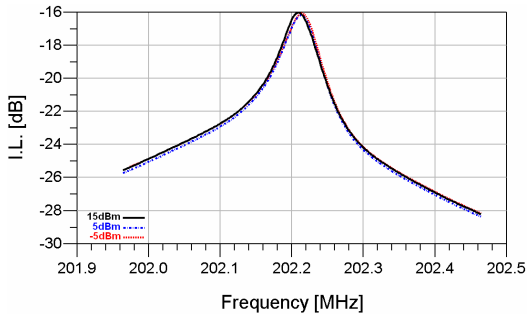

Fig. 5: Linearity measurement result for AlN-on-Si resonator

4. AMPLIFIER AND PHASE-NOISE

Transimpedance Amplifier Design

To realize a high-gain low-power broadband TIA, it is crucial to isolate the large input/output parasitic capacitance (~1.5-2pF) of the resonator. To this end, a multi-stage TIA with shunt-shunt feedback in each stage is designed (Fig. 6). This technique helps reduce the impedance of all inter-stage critical nodes; hence, increasing the frequency of these poles beyond those of the input/output. Another advantage is the elimination of on-chip inductors typically used in high-gain gigabit CMOS TIA circuits for bandwidth enhancement. The inductor elimination results in significant area reduction.

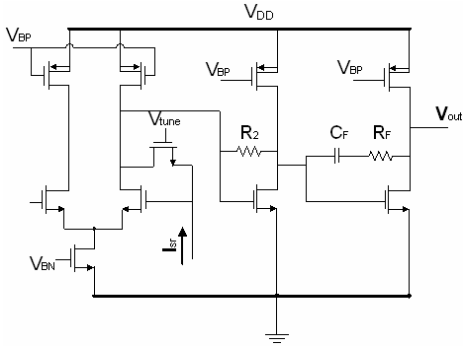

Fig.6: Schematic of the sustaining circuitry

To boost the gain at higher frequencies, capacitive coupling is used in the third stage. The high pass response of the third stage significantly attenuates the low frequency noise of the amplifier, which is higher in CMOS circuits due to large flicker noise. Therefore, the contribution of TIA noise to the overall close-to-carrier phase-noise is reduced. The choice of capacitor C_F determines the attenuation.

The resulting TIA achieves the -3dB bandwidth of more than 880MHz at maximum gain (72dB) when loaded with 2pF capacitance load at the input and output.

Oscillator Phase-Noise

The phase-noise of the oscillator can be categorized into three regions: close-to-carrier (f_{off} <20 kHz), intermediate (20 kHz < f_{off} <400 kHz), and far-from-carrier (f_{off} > 400 kHz). The dominant factor in determining close-to-carrier phase-noise of both oscillators is the Q of the resonator. Assuming a simple lumped RLC electrical model for the resonator, the phase-noise of the oscillator in close-to-carrier and intermediate region can be approximated [8] as

$$L(f_{off}) = \frac{FkT_0}{2P_o}\left[1+\frac{1}{f_m^2}\left(\frac{f_{off}}{2Q_L}\right)^2\right]\left(1+\frac{f_\alpha}{f_m}\right) \quad (1)$$

where f_m, f_{off}, f_α, F, P_o are the oscillation frequency, offset frequency, a constant related to 1/f noise corner, noise figure of the TIA, and oscillation power, respectively. Q_L, called loaded Q, is defined as

$$Q_{loaded} = Q_{unloaded}\frac{R_m}{R_m + R_{in} + R_{out}} \quad (2)$$

where Q_{UL}, R_m, R_{in}, R_{out} are unloaded Q of the resonator, motional impedance of the resonator, input, and output resistance of the TIA, respectively. Since motional impedances are roughly the same for both resonators and the center frequencies are close (which causes the input/output impedance of the TIA to be roughly the same), Q_{loaded} for AlN-on-silicon oscillator will be twice as much of that of the ZnO-on-NCD oscillator.

The phase-noise in the intermediate region is greatly influenced by the up-conversion of thermal noise of the TIA. It can be seen that the phase-noise is inversely proportional to Q_L^2. The third region shows the phase-noise floor of the oscillator that is limited by the TIA and 50Ω buffer noise.

5. MEASUREMENT RESULTS

The sustaining circuitry is fabricated in a 1P6M 0.18µm CMOS process and consumes 9.4mW. The area used by active components is 450µm×330µm (Fig. 7).

The TIA and resonators are interfaced through wirebond. An off-chip 50-ohm buffer is used to drive the measurement equipment. The output powers are 1.9dBm and 2.0dBm for 467MHz and 496MHz oscillators, respectively (Fig. 8, 9). The temperature drift of the 467MHz oscillator was measured by varying the oscillator temperature in an oven from -5 ^{O}C to 90 ^{O}C. The temperature drift was measured to be 375ppm, which corresponds to less than -4ppm/ºC (Fig. 8).

The phase-noise of both oscillators is measured with an Agilent E5500 phase-noise measurement system. The phase-noise of 467MHz ZnO-on-nanocrystalline diamond oscillator measures -80dBc/Hz at 1kHz offset with floor approaching -148dBc/Hz. The 496MHz AlN-on-Silicon oscillator exhibits phase-noise less than -92dBc/Hz at 1kHz offset with floor below -147dBc/Hz (Fig. 9).

The close-to-carrier performance of an oscillator is closely dependent to Q, however, as discussed in section 3, due to thinner substrate in ZnO-on-NCD resonator, the power handling of the 467MHz oscillator is worse than that of the 496MHz oscillator, i.e. 1.9dBm is closer to nonlinear threshold of the ZnO-on-NCD resonator. This has negative impact on the close-to-carrier phase-noise

performance. As described in section 2, the close-to-carrier phase-noise of 467MHz oscillator will be ~6dB worse than that of the 496MHz oscillator. Additional 5-6dB degradation in phase-noise is attributed to the nonlinearity phenomenon. Specifications of both oscillators are summarized in Table 1.

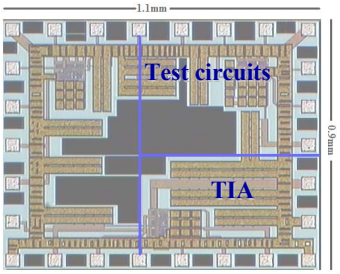

Fig. 7: Micrograph of the fabricated die

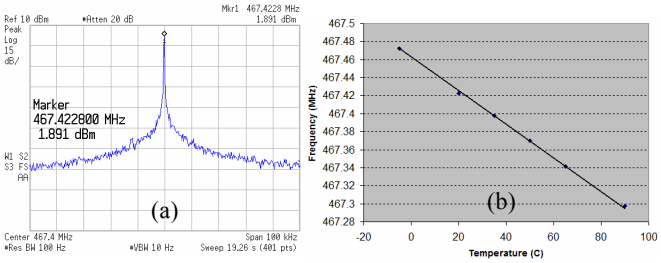

Fig. 8: (a) Spectrum and (b) TCF of 467MHz oscillator

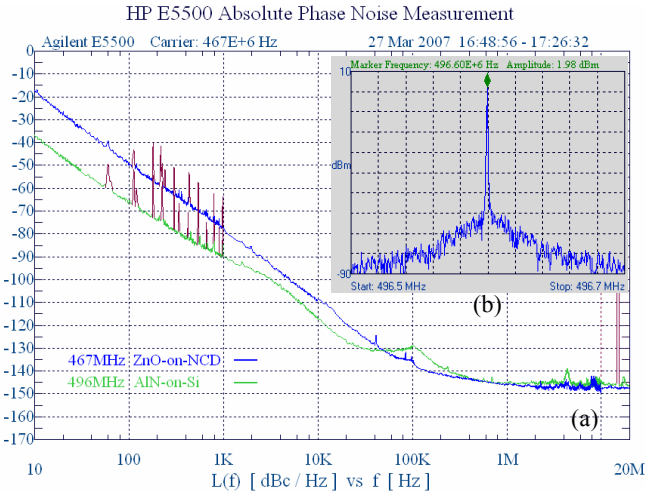

Fig. 9: (a) phase-noise performance of 467MHz and 496MHz oscillators, (b) 496MHz oscillation spectrum.

Table 1: Spec of 467MHz and 496MHz oscillators

Specification	467MHz	496MHz
Technology	AlN-on-Si	ZnO-on-NCD
Resonator Q (unloaded)	1,850	3,800
Resonator motional imp. (Ω)	600	650
Phase-noise @1kHz (dBc/Hz)	-80	-92
Phase-noise floor (dBc/Hz)	-148	-147
Power consumption (mW)	9.4	9.4
IC process	0.18µm CMOS	

6. CONCUSION

A 467MHz temperature-compensated oscillator based on a ZnO-on-nanocrystalline diamond resonator is reported for the first time. The performance of this oscillator is compared with an uncompensated 496MHz oscillator that uses an AlN-on-silicon resonator with higher unloaded Q. An inductorless high-gain broadband TIA has been designed and fabricated in 0.18µm CMOS to interface with the resonator. The power handling of both resonators and its effect on the phase-noise performance of the oscillators are studied.

7. ACKNOWLEDGEMENT

The authors thank MOSIS for IC fabrication support and Dr. James Butler from Naval Research Laboratory for providing NCD films.

REFERENCES

[1] K. Sundaresan, G. K. Ho, S. Pourkamali, and F. Ayazi, "A Low Phase Noise 100MHz Silicon BAW Reference Oscillator", in *Proc. IEEE CICC*, pp. 841-844, Sep. 2006.

[2] S. Lee, M.U. Demirci, and C.T.-C. Nquyen, "Series-Resonant VHF Michromechanical Resonator Reference Oscillators", *IEEE J. Solid-State Circuits*, vol. 39, no. 12, pp. 2477-2491, Dec 2004.

[3] H. M. Lavasani, R. Abdolvand, and F. Ayazi, "A 500MHz Low Phase-Noise AlN-on-Silicon Reference Oscillator", *in Proc. IEEE CICC*, pp. 599-602, Sep. 2007.

[4] R. Abdolvand, G. K. Ho, J. Butler, and F. Ayazi, "ZnO-on-nanocrystalline diamond lateral bulk acoustic resonators," in *Proc. 20th IEEE International Conference on Micro Electro Mechanical Systems (MEMS 2007)*, Kobe, Japan, Jan. 2007, pp. 795-798.

[5] J. B. Lee, S. H. Kwak, H. J. Kim, "Effects of surface roughness of substrates on the *c*-axis preferred orientation of ZnO films deposited by r.f. magnetron sputtering," *Thin Solid Films*, Vol. 423, Issue 2, pp. 262-266, Jan. 2003.

[6] G. K. Ho, R. Abdolvand, and F. Ayazi, "High Order Composite Bulk Acoustic Resonators," *Proc. 20th IEEE International Conference on Micro Electro Mechanical Systems (MEMS 2007)*, Kobe, Japan, Jan. 2007, pp. 791-794.

[7] V. Kaajakari, T. Mattila, A. Oja, H. Seppa, "Nonlinear limits for single-crystal silicon microresonators," *J. Microelectromech. Syst.,* Vol. 13, no. 5, pp. 715-724, Oct. 2004.

[8] G. K. Ho, K. Sundaresan, S. Pourkamali, and F. Ayazi, "Low-motional-impedance highly-tunable I2 resonators for temperature-compensated oscillators", in *Proc. 18th IEEE International Conference on Micro Electro Mechanical Systems (MEMS 2005)*, pp. 116-120, Jan 2005.